Endocrine, *vol. 26, no. 1, 25–32, February 2005* 0969–711X/05/26:25–32/$30.00 © 2005 by Humana Press Inc. All rights of any nature whatsoever reserved.

Retinoid-Related Receptor (ROR) α mRNA Expression Is Altered in the Brain of Male Mice Lacking All Ligand-Binding Thyroid Hormone Receptor (TR) Isoforms

Nandini Vasudevan,[1,*] Hosein Kami Kia,[1,*] Maria Hadjimarkou,[2,*] Noriyuki Koibuchi,[3] William W. Chin,[4] Douglas Forrest,[5] Bjorn Vennstrom,[6] and Donald Pfaff[1]

[1]Laboratory of Neurobiology and Behavior, The Rockefeller University, 1230, York Ave, New York, NY 10021; [2]Neuropsychology Program, Department of Psychology, Queens College/CUNY, 65-30 Kissena Blvd, Flushing, NY 11367; [3]Dokkyo University School of Medicine Mibu, Tochigi 321-0293 Japan; [4]Lilly Corporate Center, Building 98c/2, Room 2370, Indianapolis, IN 46285; [5]Department of Human Genetics, Mount Sinai School of Medicine, New York, NY 10029 (Current address: National Institutes of Health, NIDDK, CEB, Bldg. 10, 10 Center Drive, MSC 1770, Bethesda, MD 20892-1770); and [6]Laboratory of Developmental Biology, CMB, Karolinska Institute, Stockholm, S-17 177, Sweden

In the vertebrate brain, the thalamus serves as a relay and integration station for diverse neuronal information en route from the periphery to the cortex. Deficiency of TH during development results in severe cerebral abnormalities similar to those seen in the mouse when the retinoic acid receptor (ROR)α gene is disrupted. To investigate the effect of the thyroid hormone receptors (TRs) on RORα gene expression, we used intact male mice, in which the genes encoding the α and β TRs have been deleted. *In situ* hybridization for RORα mRNA revealed that this gene is expressed in specific areas of the brain including the thalamus, pons, cerebellum, cortex, and hippocampus. Our quantitative data showed differences in RORα mRNA expression in different subthalamic nuclei between wild-type and knockout mice. For example, the centromedial nucleus of the thalamus, which plays a role in mediating nociceptive and visceral information from the brainstem to the basal ganglia and cortical regions, has less expression of RORα mRNA in the knockout mice (–37%) compared to the wild-type controls. Also, in the dorsal geniculate (+72%) and lateral posterior nuclei (+58%) we found more RORα mRNA in dKO as compared to dWT animals. Such differences in RORα mRNA expression may play a role in the behavioral alterations resulting from congenital hypothyroidism.

Key Words: Thalamus; thyroid hormone; orphan receptor; retinoid-related receptor.

*The first three authors contributed equally to this work.

Received December 16, 2004; Revised January 20, 2005; Accepted January 24, 2005.

Author to whom all correspondence and reprint requests should be addressed: Dr. Nandini Vasudevan, Pennsylvania State University, 208, Mueller Labs, University Park, PA 16802. E-mail: nuv1@psu.edu

Introduction

Thyroid hormone is critical for growth and in the maintenance of homeostasis in homeotherms. In mammals, the thyroid hormone receptors (TRs) are important in mediating thyroid hormone effects on several physiological processes such as lipogenesis, lipolysis, and thermogenesis *(1)*. TRs belong to the nuclear receptor superfamily, members of which are characterized by a modular, domain structure *(2,3)*. In the absence of ligand, the TRs bind consensus enhancer elements called thyroid response elements (TREs) in the promoters of target genes *(4)* and repress basal transcription *(4–7)*. However, on binding the ligands, triiodothyronine (T3) or thyroxine (T4), the TRs usually function as a ligand-dependent transcription factor and activate or suppress transcription of target genes *(1,5,6,8,9)*.

The TR: Isoform Specificity and Functions in the Brain

The thyroid hormone receptor (TR) α and TRβ genes give rise to several isoforms. The TRα1 and TRα2 proteins arise as a consequence of differential splicing, although only the former binds thyroid hormone. The TRβ1 and TRβ2 isoforms have distinct N-terminal domains, whereas the DNA and ligand-binding regions are identical *(10,11)*. Lack of thyroid hormone during development leads to cretinism, characterized by mental retardation and loss of neural development *(12)*. Despite the importance of thyroid hormones in neurogenesis, relatively few functional targets of thyroid hormone in the brain have been identified *(13–17)*.

Thyroid hormones may have an effect on the expression of the retinoid-related orphan nuclear receptor in the cerebellum. The arborization of Purkinje cells (PC) in the cerebellum is possibly regulated by thyroid hormone *(18–21)*. This is underscored by the fact that in hypothyroidism the morphology of the PC and their dendritic arborization changes *(22)*. The mutant mouse *staggerer* presents a phenotype similar to that seen with hypothyroid animals. In the *staggerer* (*sg*) mutant *(23)* the PC fails to form synapses with granule

cells, leading to granule cell death *(24–26)*. As with hypothyroidism *(27–29)*, PC arborization and dendritic spine formation is also affected *(30,31)*. It was later shown that the *sg* mutation is due to the loss of the retinoid-related orphan nuclear receptor (ROR) α *(32,33)*. Hence, both lack of thyroid hormone and RORα have similar phenotypic consequences in the cerebellum.

The ROR Subfamily

The ROR subfamily consists of three related receptors, RORα, RORβ, and RORγ *(34,35)*. These receptors bind as monomers to a consensus ROR element (RORE) comprised of a half site 5' AGGTCA 3' motif preceded by an AT rich sequence *(36*, and references therein). Four isoforms, RORα1, α2, α3, and α4, generated through alternative splicing and promoter usage of the RORα gene, differ in amino termini and in DNA-binding properties *(34)*. Ontogeny of these isoforms reveals a spatiotemporal pattern of expression in the normal rat brain *(37)* and adult mouse brain *(35)*. In the mouse cerebellum, both RORα1 and RORα4 are expressed *(38)*.

Interactions Between TR and RORα in the Brain

During brain development, both TR and ROR appear to have several common targets such as the Purkinje cell protein (PCP-2) in the cerebellum *(1,39–41)*, the oxytocin gene *(42)*, and the ubiquitously expressed laminin B1 gene *(43)*. Because the hypothyroid state and the *sg* mutant have similar phenotypic abnormalities, Koibuchi and Chin speculated that RORα itself may be a downstream thyroid hormone target *(44)* via the TRs. In hypothyroid animals given thyroxine (T4) replacement, RORα mRNA in the cerebellum was increased by postnatal day 15 (P15). These data indicate that thyroid hormone plays an important part in the developmental regulation of RORα *(44)*, possibly via TRs. To explore further the hypothesis that TR plays a role in the regulation of ROR4 transcription in adult mice, we determined the TR-controlled basal expression of the RORα gene in mice devoid of all ligand-binding TR isoforms (dKO).

Results

The distribution of cells which hybridized to the RORα probe in the present study was the same as those described in rat brain *(37)* and in the mouse brain *(35)*. Gross macroscopic observations of the brain of TR $\alpha1^{-/-}$ $\beta^{-/-}$ mice did not show major abnormalities when compared to control TR $\alpha1^{+/+}$ $\beta^{+/+}$ animals. Moreover, histological observation during sectioning did not reveal major abnormalities in the white-gray matter ratio, relative to the major white tracts used as anatomical landmarks (corpus callosum, anterior commissure, fimbria-fornix).

The sagittal sections reveal the same pattern of RORα mRNA distribution in TR $\alpha1^{-/-}$ $\beta^{-/-}$ (dKO) when compared to wildtype controls. In the sagittal sections, the RORα mRNA containing cells were detected in the pons, cerebral cortex, piriform cortex, thalamus, inferior colliculus, superior colliculus, and cerebellum (Figs. 1A and 2A). In the same sagittal plane, no evidence of RORα transcript was found in the striatum (Figs. 1A and 2A). In the telencephalon, the largest number of the RORα mRNA containing cells in dKO and dWT were localized in the piriform cortex and the cerebral cortex (Figs. 1B, 2B and Table 1).

Our quantitative hybridization data, performed by using coronal sections, showed that a low expression of RORα mRNA could be detected in the CA1–CA3 layer of the hippocampus and the dentate gyrus (DG) (Figs. 1B,C and 2B, C) in both wild-type controls and knockout mice. At the same level as the hippocampus, high expression of RORα mRNA could be seen in all subthalamic nuclei. Among the different subthalamic nuclei, the geniculate nucleus (the dorsal lateral area) (+72%), the lateral posterior thalamic (rostral area) nucleus (+58%), and the posterior thalamic nuclear group (+18%) showed higher levels of RORα mRNA expression in the dKO compared to the dWT animals (Figs. 1B,C and 2B,C, Figs. 3A,B, and Table 1). Conversely, in the mediodorsal thalamic (+63%) (Figs. 3C,D) and the centromedial (+37%) thalamic nuclei, the RORα mRNA levels were higher in the dWT compared to the dKO (Table 1) animals. In the midbrain, the superior colliculus in the dWT showed slightly higher RORα mRNA expression compared to the dKO animals (Figs. 1D and 2D and Table 1). In the inferior colliculus, we found a moderate signal in both dKO and dWT animals (Fig. 1A and 2A respectively). At the same level, moderate expression of the RORα transcript could be detected in the retrosplenial cortex in both genotypes (Figs. 1D and 2D). However, in the medial geniculate nucleus, dKO animals expressed less RORα mRNA compared to dWT (Figs. 1D and 2D and Table 1) animals. In the myelencephalon, a strong *in situ* hybridization signal was observed in the cerebellum (Figs. 1E and 2E). Our quantitative analysis revealed no differences in RORα mRNA expression in dKO animals compared to dWT mice in the cerebellum (Table 1).

Discussion

Distribution of RORα mRNA in the Mouse Brain

The RORα mRNA expression is widespread throughout the mouse brain. In the telencephalon, RORα mRNA was seen in the dentate gyrus and in the hippocampus. In the mesencephalon and metencephalon, RORα expression was widely distributed in the periaqueductal gray, the cerebellum, and the superior colliculus. The RORα expression is particularly intense in the thalamic nuclei. This is in general agreement with the distribution reported previously in the adult mouse brain *(35)*.

Differences Between the dKO and the dWT Mice: Expression of RORα

The thalamus is required for the integration of sensorimotor information and is critical for the relay of informa-

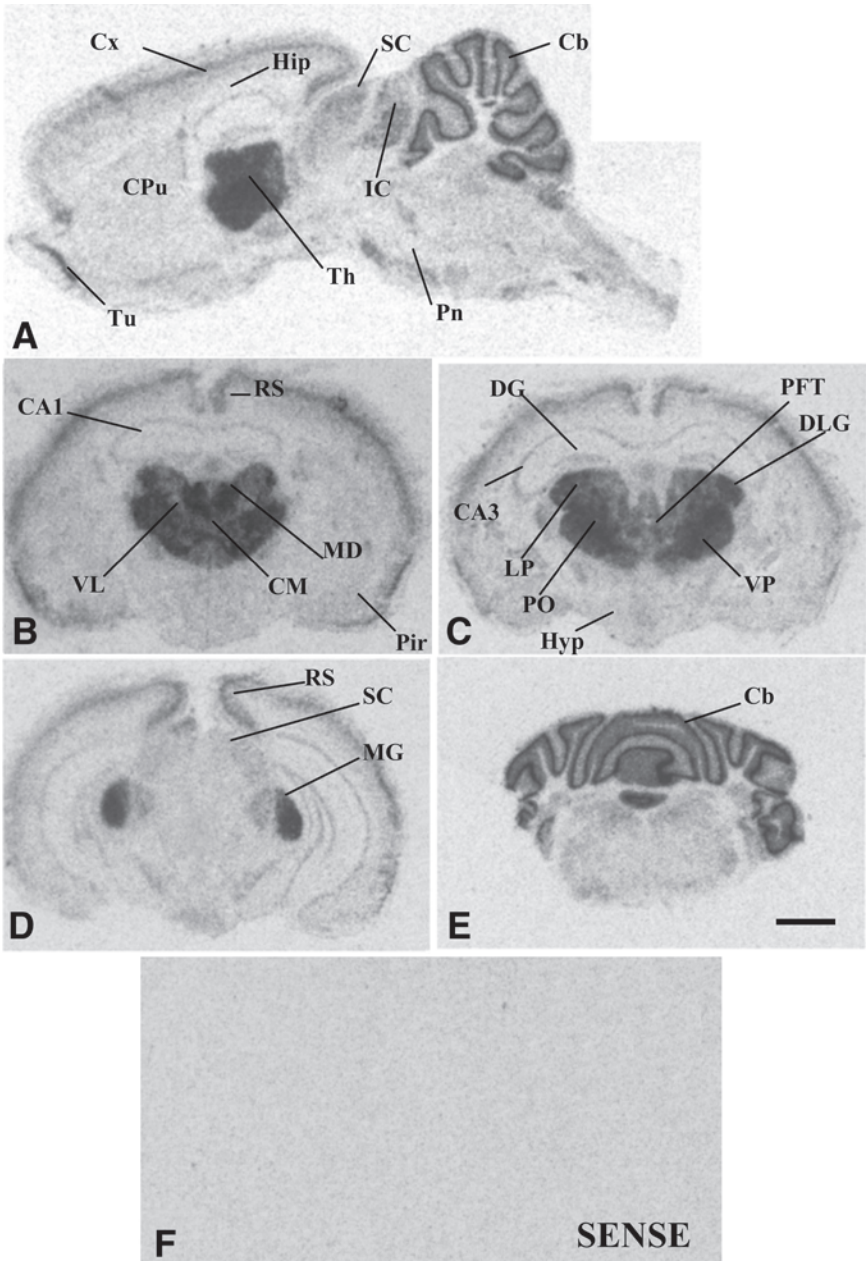

Fig. 1. Film autoradiography showing the distribution of RORα mRNA in the brain of the adult dWT male mouse. Gonadally intact adult wild-type mice were sacrificed and 12 μm coronal sections were hybridized to ^{35}S-UTP-labeled RORα mRNA at 62°C. After high stringency washes and progressive dehydration with alcohol, the sections on slides were exposed to BioMax Film for 5 d. Optical density analysis was done from three to four matched coronal sections/animal of RORα mRNA expression in subnuclei using MCID software. For every nuclei, Student's *t*-test ($p < 0.05$ considered significant) was used to compare RORα mRNA between dKO and dWT. (**A**) The expression of RORα mRNA in a sagittal section. The majority of RORα transcript-containing cells were localized in the diencephalon especially in the thalamus region. (**B–E**) The distribution of RORα mRNA in progressive coronal sections from the rostral to caudal axis (**B–E**) in the brain of the adult male dWT mouse. Panels **B** and **C** represent thalamic and limbic regions. Panel **D** details the RORα mRNA expression in the midbrain. Panel **E** shows the expression of RORα mRNA in the cerebellum. No signal was detected in the sagittal section, which was labeled with a sense probe (Panel **F**). Scale bar, 5 mm. Abbreviations: CA1–CA3, fields of hippocampus; Cb, cerebellum; CM, central medial thalamic nucleus; Cx, cortex; CPu, caudate-putamen (striatum); DG, dentate gyrus; DLG, dorsal lateral geniculate nucleus; Hip, hippocampus; Hyp, hypothalamus; IC, inferior colliculus; LP, lateral posterior thalamic nucleus; MG, medial geniculate nucleus; PFT, parafascicular thalamic nucleus, Pir, piriform cortex; Pn, pons; PO, posterior thalamic nuclear group; RS, retrosplenial cortex; SC, superior colliculus; Th, thalamus; Tu, olfactory tubercle; VL, ventrolateral thalamic nucleus; VP, ventroposterior thalamic nucleus.

tion from the somatosensory and the motor cortices *(45)*. The expression of RORα in the lateral and medial thalamic nuclei differs in the knockout mouse compared to the wild-type controls. However, the type of effect of the TR deletion is region specific. In the lateral nuclei such as the lateral posterior thalamus and the geniculate nucleus, the RORα

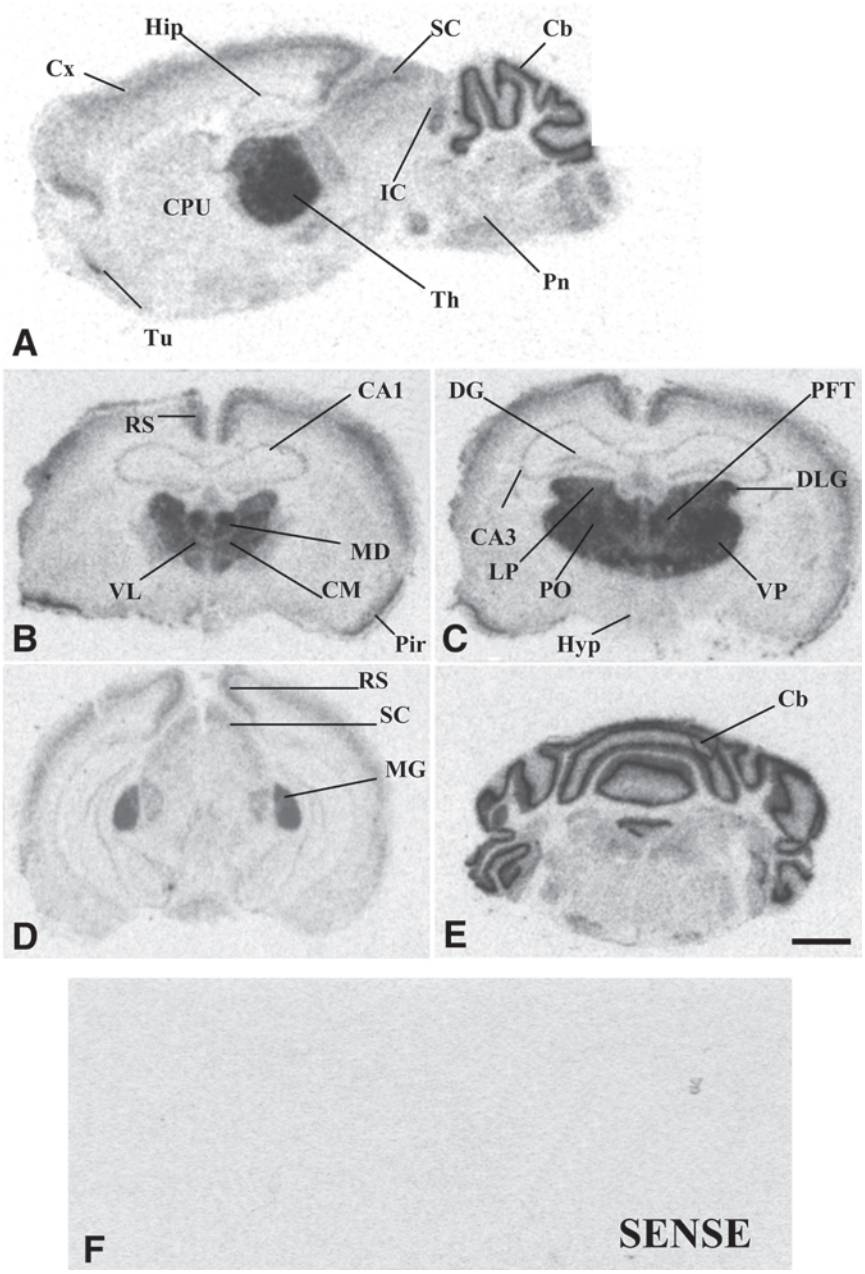

Fig. 2. Film autoradiography showing the distribution of RORα mRNA in the brain of the adult dKO male mouse. Methods are as detailed in Fig. 1. (**A**) The expression of RORα mRNA in a sagittal section. As in the dWT mouse, the majority of RORα mRNA-containing cells were localized in the thalamus region. (**B–E**) The distribution of RORα mRNA in progressive coronal sections (n = 3–4 matched coronal sections/animal) from the rostral to caudal axis in the brain of the adult male mouse. Panels **B** and **C** represent thalamic and limbic regions. Panel **D** details the RORα mRNA expression in the midbrain. Panel **E** shows the expression of RORα mRNA in the cerebellum. No signal was detected in the sagittal section, which was labeled with a sense probe (Panel **F**). Scale bar, 5 mm. Abbreviations: CA1–CA3, fields of hippocampus; Cb, cerebellum; Cx, cortex; CPu, caudate-putamen (striatum); DG, dentate gyrus; DLG, dorsal lateral geniculate nucleus; Hip, hippocampus; Hyp, hypothalamus; IC, inferior colliculus; LP, lateral posterior thalamic nucleus; MG, medial geniculate nucleus; PFT, parafascicular thalamic nucleus, Pir, piriform cortex; Pn, pons; PO, posterior thalamic nuclear group; RS, retrosplenial cortex; SC, superior colliculus; Th, thalamus; Tu, olfactory tubercle; VL, ventrolateral thalamic nucleus; VP, ventroposterior thalamic nucleus.

expression is higher in the knockout mouse. The posterior group nuclei, particularly the VPL, are the synapses for afferents, which ascend into the somatosensory cortex. On the other hand, in the medial nuclei such as the medial dorsal thalamus (central and lateral parts), there is lower RORα mRNA expression in the knockout as compared to wild type.

The Expression of RORα in the Motor Circuit is Affected by the Lack of Ligand-Binding TR

In this study, we demonstrate that RORα mRNA in an area critical for sensory and motor control, the thalamus, is affected by the lack of TRs. This study does not allow us to distinguish if these are direct consequences of the lack of

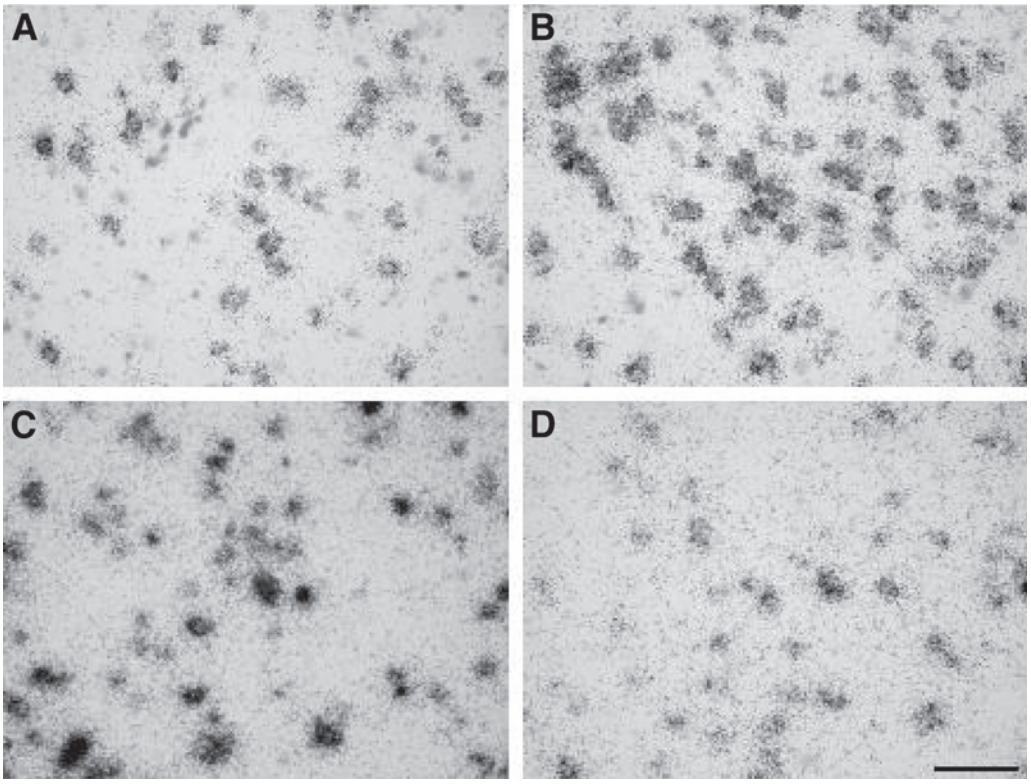

Fig. 3. Representative brightfield photomicrographs of RORα mRNA expression in the dorsal lateral geniculate nucleus in the dWT (**A**) and in the dKO (**B**) mouse. Photomicrographs **C** and **D** show RORα *in situ* hybridization in the mediodorsal thalamic nucleus of the dWT and dKO mice respectively. Note the level of expression of the RORα mRNA in the WT and KO animals. Scale bar, 25 μm.

Table 1
Optical Density Measurements of RORα mRNA From Film Autoradiograms/Stained Slides in dKO and dWT Adult Male Mice[a]

Region	$TR\alpha1^{+/+}\ \beta^{+/+}$ (optical density)	$TR\alpha1^{-/-}\ \beta^{-/-}$ (optical density)
CA1	0.09 ± 0.01	0.08 ± 0.01
CA2–CA3	0.11 ± 0.01	0.12 ± 0.01
DG	0.13 ± 0.01	0.11 ± 0.01
DLG	0.64 ± 0.04*	1.10 ± 0.05
MG	0.83 ± 0.01	0.64 ± 0.02*
LPT	0.60 ± 0.03*	0.95 ± 0.06
MDT	0.93 ± 0.02	0.53 ± 0.05*
CM	0.49 ± 0.02	0.31 ± 0.03*
VP	0.87 ± 0.02	0.86 ± 0.01
Pons	0.85 ± 0.02*	1.01 ± 0.06
SC	0.34 ± 0.02	0.21 ± 0.03*
IC	0.35 ± 0.01	0.41 ± 0.04
RS	0.35 ± 0.01	0.41 ± 0.05
Cortex	0.51 ± 0.04	0.45 ± 0.02
Piriform Cx	0.51 ± 0.03	0.53 ± 0.03

[a]Values represent mean ± SEM of three or four sections per mouse. The asterisk denotes nuclei, which show a lower RORα expression when compared to the same nuclei in the other genotype. Abbreviations: CA1-CA3, fields of hippocampus; DG, dentate gyrus; DLG, dorsal lateral geniculate nucleus; IC, inferior colliculus; LPT, lateral posterior thalamic nucleus; MDT, mediodorsal thalamic nucleus; MG, medial geniculate nucleus; CM, central medial thalamic nucleus; RS, retrosplenial cortex; SC, superior colliculus; VP, ventroposterior thalamic nucleus.

ligand-binding TRs or an indirect, related effect. The motor system is affected both by the hypothyroid state and by mutations in the RORα gene (*sg* mutant), principally by affecting the PC in the cerebellum *(23)*. The sluggishness seen in the hypothyroid state *(46–48)* may therefore be a manifestation of these thalamic changes. However, although these data may indicate a motor deficit in the dKO mouse model, there have been no defects in the motor system reported in the dKO to date. This is in agreement with previous studies reporting the absence of differences between hypothyroid and euthyroid animals in RORα mRNA expression in the PC of the adult mouse *(44)*. It is possible that such a difference in the cerebellum between the hypothyroid and euthyroid state is only seen during early postnatal development, where there is a critical "window" for thyroid hormone action *(19,44,49,50)* or that there is compensation for the loss of the ligand-binding TR isoforms. Hence, the functional consequence of differential changes in RORα mRNA in specific thalamic areas in the male adult mouse is not clear.

The Differences Between dKO and the Wild Type also Occur in the Visual Pathway

Two areas involved in the processing of visual cues also show differences in RORα mRNA expression. Mice lacking TRβ2 lack green cone photoreceptors *(51)*. In the lateral geniculate nuclei, which relay visual information from the optic nerve fibers into the primary visual cortex, the RORα mRNA is higher in the dKO than in the wild-type animals. On the other hand, RORα mRNA expression is lower in the dKO in the superior colliculus, which is needed for processing unconscious visual input from the retina and in controlling orienting behaviors *(45)*. Again, no deficits in such behaviors have been reported in the dKO.

It is therefore possible that both motor and visual behaviors may not be directly regulated by the TRs and that the lack of ligand-binding TRs may not mirror the phenotypes seen in the hypothyroid state.

This study shows for the first time the alteration of expression of the retinoid-related orphan receptor, RORα, in mice that lack ligand-binding TRs. Because targets of RORα in the brain are poorly determined, the significance of differential regulation of this nuclear receptor in various brain regions is not clear. RORα can also mediate repression and activation of genes in a manner similar to thyroid hormone *(36)*. Therefore, differential regulation of RORα by TR in different brain areas may represent a mechanism whereby the same downstream genes can be regulated differentially to ensure flexible gene regulation.

Methods and Materials

Animals

The double knockout mice (dKO) lack TRα1 and both TRβ isoforms and hence do not possess any ligand-binding TR. They are derived from the TRα1 and TRβ knockout mice by heterozygote crosses *(52,53)*. The genetic background of the TRα1 mice is the 129OlaHsd × BALB/C and that of the TRβ knockout mice is the 129/Sv × C57BL/6J. Gonadally intact, male mice were isolated by genotype and housed in plastic cages (30 cm × 20 cm × 13 cm). Water and food were provided *ad libitum*. They were housed in a room on a reversed 12 h light: 12 h dark cycle (lights off at 10 AM). The genotypes were determined by polymerase chain reaction from genomic DNA extracted from mouse tail.

Tissue Collection

Gonadally intact, adult WT and KO male mice (12–16 wk of age; $n = 4$/genotype) were used for the experiments. Procedures for sacrifice were approved by the University Animal Use Committee. Mice were quickly exposed to a lethal dose of CO_2 and decapitated. On rapid removal of brains, isopentane at −30°C was used to freeze the brains. The brains were then stored at −80°C until sections could be made. A series of coronal sections (12 μm) of the whole brain from the olfactory bulb to the brain stem were cut in a cryostat and thaw mounted onto SuperFrost®Plus slides (Fisher, Inc, Pittsburgh, PA). These slides were air dried and then kept at −80°C until use.

Plasmids and Probe Preparation

The plasmid expressing RORα receptor was described previously *(44)*. The probe was labeled by in vitro transcription with ^{35}S-UTP (>1000 Ci/mmol; NEN), using SP6 (antisense) and T7 (sense) polymerases. The ^{35}S-labeled probes were purified on G50-Sephadex Quick Spin® columns (Roche) and precipitated in absolute ethanol. The specificity of this probe has been shown previously *(44)*.

In Situ *Hybridization Procedure (Detection of ^{35}S-Labeled Probes)*

The protocol for *in situ* hybridization has been previously described *(54)*. Briefly, slides were removed carefully from the −80°C and quickly fixed, acetylated, and progressively dehydrated. They were then hybridized overnight at 62°C with RORα cRNA *(55)* labeled probes (2 × 106 cpm of ^{35}S probe in 100 μL of hybridization solution). The hybridization solution was as follows: 50% formamide, 10% dextran sulfate, 20 m*M* Tris-HCl pH 8.0, 5 m*M* EDTA pH 8.0, 0.75 *M* NaCl, 250 m*M* dithiotheritol, 0.1% sodium dodecyl sulfate, 1X Denhardt's/250 μg/mL yeast tRNA. At the end of the hybridization, the slides were washed using high stringency washes and treated with RNase A (20 μg/mL, Boehringer-Mannheim) at 37°C for 45 min. After a series of progressive dehydrations in alcohol, the slides were exposed to BioMax MR film (Kodak) for 4–5 d. All autoradiographic films were developed and processed for analysis at identical time points. The specificity of the hybridization reaction was confirmed because *in situ* hybridization of sections with sense probe, or sections pretreated with RNase A prior to hybridization with the antisense probe, showed no specific signal.

Analysis and Quantification

Neuroanatomical subdivisions were determined using the atlas of Franklin and Paxinos *(56)*. The film autoradiograms (which were developed at identical time points to avoid interassay variability) were analyzed using a computer-assisted microdensitometry system (MCID, Imaging Research, St Catharine's, Ontario, Canada). Slides undergoing hybridization were stained and used to aid in the determination of nuclear boundaries, particularly within the thalamic nuclei where the division between the different subnuclei is readily discernible from stained material. An observer who was unaware of the identity of the genotypes being examined performed the analysis. Optical density values were obtained from three or four carefully matched coronal sections per animal, structures were delineated interactively, and pixel gray levels were measured in the outlined areas. Gray level/optical density calibrations were performed using a calibrated film strip (Imaging Research) for optical density. In order to correlate optical density with amount of radioactivity, ^{14}C (ARC, St Louis, Mo, USA) standards strips were co-exposed with the experimental sections. The gray levels that produced optical densities within a linear function were quantified in the samples and optical densities outside the linear range were not used. Background radioactivity values were measured in each structure on the negative control sections, i.e., sections hybridized with sense probe. Specific labeling was calculated by subtracting background radioactivity levels measured from the same region on the adjacent negative control section. For analysis, we focused our attention on the structures which show an important expression of RORα mRNA such as pons, cerebral cortex, piriform cortex, retrosplenial cortex, hippocampus (CA1–CA3), dentate gyrus, the thalamic nuclei, the superior colliculus, the inferior colliculus, and the cerebellum. Statistical analysis comparing the knockout mice with their wild-type counterparts was carried out by Student's *t*-test. In all instances $p < 0.05$ was considered statistically significant. In cases where there was a significant difference in subnuclei between the dWT and dKO animals, the optical density of that region in the dWT was arbitrarily set at 100% and the optical density for that region in the dKO was compared to this 100% set point. This is reported in the abstract.

The slides were dipped in NTB-2 (Kodak) emulsion for single-cell emulsion autoradiographic analysis for 3–4 wk at 4°C in the dark. They were then developed in D19 developer (Kodak), rinsed in MilliQ water, and fixed in rapid fixer (Kodak). The slides were rinsed and counterstained with methylene blue, dehydrated, cleared in xylene, and coverslipped with DPX (Electron Microscopy Sciences).

Photomicrography

Bright field photomicrographs were produced by capturing images with a digital camera (AxioCam, Zeiss) mounted directly on the microscope (Zeiss Axioscop2). A Gateway PC computer running Adobe Photoshop was used to assemble composite photomicrographs.

Acknowledgments

We thank Dr. Bruce McEwen and his lab members as well as Dr. Masayoshi Nomura for their assistance with image analysis. This work was supported by NIH grant HD-05751 to Dr. Donald Pfaff. D.F. is supported by a Hirschl Award, the March of Dimes Birth Defects Foundation, and the NIH (DC-03441). B.V. received support from The Swedish Cancer Society and Karobio AB.

References

1. Oppenheimer, J. H., Schwartz, H. L., and Strait, K. A. (1995). In: *Molecular endocrinology: basic concepts and clincal correlations*. Weintraub, B. (ed.). Raven Press: New York.
2. Lazar, M. (1993). *Endocrine Rev.* **14,** 184–193.
3. Zhang, J. and Lazar, M. A. (2000). *Annu. Rev. Physiol.* **62,** 439–466.
4. Sap, J., Munoz, A., Schmitt, J., Stunnenberg, H., and Vennstrom, B. (1989). *Nature* **340,** 242–244.
5. Evans, R. M. (1988). *Science* **240,** 889–895.
6. Mangelsdorf, D. J., Thummel, C., Beato, M., et al. (1995). *Cell* **83,** 835–840.
7. Damm, K., Thompson, C. C., and Evans, R. M. (1989). *Nature* **339,** 593–597.
8. Feng, X., Jiang, Y., Meltzer, P., and Yen, P. M. (2000). *Mol. Endocrinol.* **14,** 947–955.
9. Flores-Morales, A., Gullberg, H., Fernandez, L., et al. (2002). *Mol. Endocrinol.* **16,** 1257–1268.
10. Chin, W. W. (1991). In: *Nuclear hormone receptors*. Parker, M. (ed.). Academic Press: New York.
11. Harvey, C. B. and Williams, G. R. (2002). *Thyroid* **12,** 441–446.
12. Delange, F. M. and Ermans, A. M. (1979). In: *The thyroid: physiology and treatment of disease*. Hershman, J. M. and Bray, G. A. (eds.). Pergamon Press: New York.
13. Bernal, J., Guadano-Ferraz, A., and Morte, B. (2003). *Thyroid* **13,** 1005–1012.
14. Morreale de Escobar, G., Obregon, M. J., and Escobar del Rey, F. (2004). *Eur. J. Endocrinol.* **151(Suppl 3),** U25–U37.
15. Forrest, D. (2004). *Endocrinology* **145,** 4034–4036.
16. Anderson, G. W., Schoonover, C. M., and Jones, S. A. (2003). *Thyroid* **13,** 1039–1056.
17. Konig, S. and Moura Neto, V. (2002). *Cell Mol. Neurobiol.* **22,** 517–544.
18. Morte, B., Manzano, J., Scanlan, T. S., Vennstrom, B., and Bernal, J. (2004). *Endocrinology* **145,** 1386–1391.
19. Morte, B., Manzano, J., Scanlan, T., Vennstrom, B., and Bernal, J. (2002). *Proc. Natl. Acad. Sci. USA* **99,** 3985–3989.
20. Heuer, H. and Mason, C. A. (2003). *J. Neurosci.* **23,** 10604–10612.
21. Koibuchi, N. and Chin, W. W. (2000). *Trends Endocrinol. Metab.* **11,** 123–128.
22. Legrand, J. and Bout, M. C. (1970). *C. R. Acad. Sci. Hebd. Seances. Acad. Sci. D.* **271,** 1199–1202.
23. Sidman, R. L., Lane, P. W., and Dickie, M. M. (1962). *Science* **137,** 610 –612.
24. Clos, J., Crepel, F., Legrand, C., Legrand, J., Rabie, A., and Vigouroux, E. (1974). *Gen. Comp. Endocrinol.* **23,** 178–192.
25. Crepel, F. (1974). *Exp. Brain Res.* **20,** 403–420.
26. Crepel, F. (1975). *Brain Res.* **85,** 157–160.
27. Nicholson, J. L. and Altman, J. (1972). *Science* **176,**
28. Nicholson, J. L. and Altman, J. (1972). *Brain Res.* **44,** 13–23.

29. Rabie, A., Favre, C., Clavel, M. C., and Legrand, J. (1979). *Brain Res.* **161,** 469–479.
30. Herrup, K. (1983). *Dev. Brain Res.* **11,** 267–274.
31. Sotelo, C. and Changeux, J.-P. (1974). *Brain Res.* **67,** 519–526.
32. Hamilton, B. A., Frankel, W. N., Kerrebrock, A. W., et al. (1996). *Nature* **379,** 736–739.
33. Dussault, I., Fawcett, D., Matthyssen, A., Bader, J. A., and Giguere, V. (1998). *Mech. Dev.* **70,** 147–153.
34. Giguere, V., Tini, M., Flock, G., Ong, E., Evans, R. M., and Otulakowski, G. G. (1994). *Genes Dev.* **8,** 538–553.
35. Matsui, T., Sashihara, S., Oh, Y., and Waxman, S. G. (1995). *Brain Res. Mol. Brain Res.* **33,** 217–226.
36. Jetten, A. M., Kurebayashi, S., and Ueda, E. (2001). *Prog. Nucleic Acid Res. Mol. Biol.* **69,** 205–247.
37. Sashihara, S., Felts, P. A., Waxman, S. G., and Matsui, T. (1996). *Brain Res. Mol. Brain Res.* **42,** 109–117.
38. Matysiak-Scholze, U. and Nehls, M. (1997). *Genomics* **43,** 78–84.
39. Matsui, T. (1997). *Genes Cells* **2,** 263–272.
40. Oppenheimer, J. H. and Schwartz, H. L. (1997). *Endocr. Rev.* **18,** 462–475.
41. Zou, L., Hagen, S. G., Strait, K. A., and Oppenheimer, J. H. (1994). *J. Biol. Chem.* **269,** 13346–13352.
42. Chu, K. and Zingg, H. H. (1999). *J. Mol. Endocrinol.* **23,** 337–346.
43. Matsui, T. (1996). *Biochem. Biophys. Res. Commun.* **220,** 405–410.
44. Koibuchi, N and Chin, W. W. (1998). *Endocrinology* **139,** 2335–2341.
45. Kandel, E. R., Schwartz, J. H., and Jessel, T. M. (1991). *Principles of neural science*. Elsevier: New York.
46. Bauer, M. S. and Whybrow, P. C. (1988). *Integr. Psychiatry* **6,** 75–100.
47. Arque, J. M., Segura, R., and Torrubia, R. (1987). *Neuropsychobiology* **18,** 127–133.
48. Balada, F., Torrubia, R., and Arque, J. M. (1992). *Neuropsychobiology* **25,** 208–213.
49. Koibuchi, N., Yamaoka, S., and Chin, W. W. (2001). *Thyroid* **11,** 205–210.
50. Barradas, P. C., Vieira, R. S., and De Freitas, M. S. (2001). *J. Neurosci. Res.* **66,** 254–261.
51. Ng, L., Hurley, J. B., Dierks, B., et al. (2001). *Nat. Genet.* **27,** 94–98.
52. Göthe, S., Wang, Z., Ng, L., et al. (1999). *Genes Develop.* **13,** 1329–1341.
53. Forrest, D., Erway, L. C., Ng, L., Altschuler, R., and Curran, T. (1996). *Nat. Genet.* **13,** 354–357.
54. Kia, H. K., Krebs, C. J., Koibuchi, N., Chin, W. W., and Pfaff, D. W. (2001). *J. Comp. Neurol.* **437,** 286–295.
55. Mize, A. L. and Alper, R. H. (2000). *Brain Res.* **859,** 326–333.
56. Franklin, K. B. J. and Paxinos, G. (1997). *The mouse brain in stereotaxic coordinates*. Academic Press: San Diego, CA.